Available online at www.sciencedirect.com
SCIENCE DIRECT®
Bioorganic & Medicinal Chemistry 13 (2005) 4871–4879
Bioorganic & Medicinal Chemistry

Design, synthesis, and biological evaluation of novel naphthoquinone derivatives with CDC25 phosphatase inhibitory activity

Marie-Priscille Brun,[a] Emmanuelle Braud,[a] Delphine Angotti,[a] Odile Mondésert,[b] Muriel Quaranta,[b] Matthieu Montes,[a] Maria Miteva,[a] Nohad Gresh,[a] Bernard Ducommun[b] and Christiane Garbay[a,*]

[a]*Laboratoire de Pharmacochimie Moléculaire et Cellulaire INSERM U648—CNRS FRE 2718, UFR Biomédicale, 45 rue des Saints Pères, 75270 Paris Cedex 06, France*
[b]*Laboratoire de Biologie Cellulaire et Moléculaire du Contrôle de la Prolifération UMR 5088—IFR 109 Université Paul Sabatier, Route de Narbonne, 31062 Toulouse, France*

Received 21 March 2005; revised 27 April 2005; accepted 3 May 2005
Available online 24 May 2005

Abstract—CDC25 dual-specificity phosphatases are essential key regulators of eukaryotic cell cycle progression and the CDC25A and B isoforms are over-expressed in different tumors and related cancer cell lines. CDC25s are now considered to be interesting targets in the search for novel anticancer agents. We describe new compounds derived from vitamin K_3 that inhibit CDC25B activity with IC_{50} values in the low micromolar range. These naphthoquinone derivatives also display antiproliferative activity on HeLa cells as expected for CDC25 inhibitors and inhibit cell growth in a clonogenic assay at submicromolar concentrations. They increase inhibitory tyrosine 15 phosphorylation of CDK and induce the cleavage of PARP, a hallmark of apoptosis.

1. Introduction

The accurate transduction of intracellular signals is achieved through processes of phosphorylation–dephosphorylation of cyclin-dependent kinase (CDK) complexes, which are key regulators of essential cellular events such as cell cycle regulation, growth, or differentiation. CDKs are activated by the CDC25 dual-specificity phosphatases, which catalyze the dephosphorylation of two adjacent phosphothreonine and phosphotyrosine residues on the CDK subunit.[1,2]

Three genes expressing CDC25 have been identified in human cells, namely CDC25A, CDC25B, and CDC25C,[3–5] and several splice variants have been characterized.[6,7] CDC25A, expressed in the G1 phase, allows the progression of the cell into the S phase by dephosphorylation of the CDK2/cyclin A complex.[8–10] Microinjection of CDC25A antibodies into cells induces cell arrest by blocking G1/S transition.[8,9] It has also been suggested that CDC25A is involved in mitosis.[10] CDC25B and CDC25C are activators of Cdc2/cyclin B, Cdc2/cyclin A, and CDK2/cyclin A complexes and play a role in the G2/M transition and in the control of entry into mitosis.[11,12]

CDC25A and B have been reported to present oncogenic properties.[13] Furthermore, they are found to be over-expressed in many tumors with poor prognosis including head and neck cancers, colon cancers, non-small cell lung, and breast cancers.[14–16] Thus, the discovery of potent CDC25s inhibitors appears as an attractive approach in the search for new targeted anticancer agents.

Several classes of CDC25s inhibitors have been reported so far showing cytotoxicity in the micromolar concentration range (Chart 1). They include natural substances and their synthetic derivatives such as dysidiolide[17] or sulfiricins,[18] analogs of vitamin K_3[19,20] and D_3,[21,22] as well as naphthoquinones,[23,24] quinolinediones,[25] or

Keywords: Cancer; Signal transduction; CDC25 phosphatases; Naphthoquinones.
* Corresponding author. Tel.: +33 142 864 080; fax: +33 142 864 082; e-mail: christiane.garbay@univ-paris5.fr

0968-0896/$ - see front matter © 2005 Elsevier Ltd. All rights reserved.
doi:10.1016/j.bmc.2005.05.005

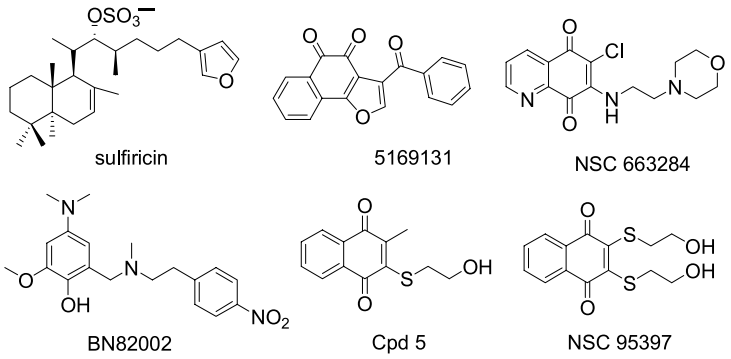

Chart 1. Inhibitors of CDC25 phosphatases.

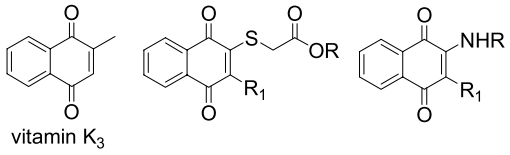

Chart 2. Chemical structures of novel vitamin K_3 derivatives.

naphthofurane-diones.[26] Recently, Brezak et al. described a new CDC25 inhibitor BN82002 (IC_{50} = 6.3 μM on CDC25B3) and its analogs.[27,28] In our search for new CDC25 inhibitors, we were interested in vitamin K_3 and its thio-analogs Cpd 5 and NSC 95397 (Chart 1). Indeed, Cpd 5 has been reported to inhibit CDC25A with an IC_{50} value of 5.6 μM in Hep3B hepatoma cells and to arrest cell cycle progression at G1 and G2/M,[29,30] whereas NSC 95397 was claimed to be one of the most potent CDC25 inhibitors with an IC_{50} value in the nanomolar range and to block the G2/M transition.[31]

The recently solved X-ray crystallographic structure of the catalytic domain of CDC25B[32] has revealed the presence of four arginine residues (Arg479, 482, 544, and 548) located in the active site of the enzyme. As the substrate is recognized by its phosphate group, we decided to introduce carboxylate groups, bioisosteres of the phosphate, to target these residues. Thus, we describe in the present paper the design and synthesis of novel derivatives of vitamin K_3 (Chart 2) as well as the biological results obtained in terms of inhibition of CDC25B3, antiproliferative activity on HeLa cells, and the effect on cell cycle progression. Since our design of carboxylic derivatives did not result in increased activity, we performed molecular modeling studies to understand the potential roles of these negatively charged groups with regard to binding affinity. Moreover, we replaced the sulfur atom by a nitrogen atom to examine the effects of a restricted conformation of the substituted alkyl chain.

2. Chemistry

The sulfur and nitrogen series were synthesized using Michael-type 1,4-addition of primary amines and thiols to 2-methyl-[1,4]-naphthoquinone or 2,3-dichloro-[1,4]-naphthoquinone, followed by subsequent air-oxidation of naphthohydroquinones to the naphthoquinone core.

The carboxylic acid **1** was obtained by nucleophilic attack of mercaptoacetic acid at position 3 of menadione in the presence of DBU following the method described by Lazo et al., applied to synthesize Cpd 5 (Scheme 1).[31] To prepare the di-acid compound **2**, which is an analog of NSC 95397, 2,3-dichloronaphthoquinone was reacted with 2 equivalents of mercaptoacetic acid, DBU being replaced by pyridine.[33] The temperature was maintained at 65 °C and **2** precipitated in high yield (89%) within 15 min (Scheme 1). We applied the same conditions to synthesize the benzyl ester **4** but in this case we did not observe the formation of a precipitate. However, monitoring the reaction by TLC revealed the presence of two major products and the heating was maintained at 65 °C for 1 h. The mono-ester **3** and the di-ester **4** were isolated after purification in, respectively, 42% and 36% yields, with a greater solubility of the ester adducts and a thermodynamic equilibration between **3** and **4** and the starting material explaining the orientation of the reaction in favor of compound **3** (Scheme 1).

In the N-substituted series, the 3-methyl compounds **5**, **6**, and **7** were obtained by addition of the corresponding primary amines to menadione whereas the chloro derivatives **8** and **9** were synthesized from 2,3-dichloro-[1,4]-naphthoquinone in the presence of the corresponding amines and triethylamine in, respectively, 46% and 59% yields (Scheme 2). Finally, the hydroxyl derivative **8** was converted into the bromo derivative **10** using mild conditions (CBr_4/PPh_3) in 72% yield (Scheme 2).[34] This compound was originally synthesized to introduce other bioisosteric groups of the phosphate such as malonate or phosphonate groups. Unfortunately, these compounds could not be obtained by this method.

3. Results and discussion

3.1. Enzymatic activity

All our compounds were evaluated for in vitro enzymatic inhibition using recombinant fused MBP-CDC25B3 (one of the identified splicing variants of CDC25B) with

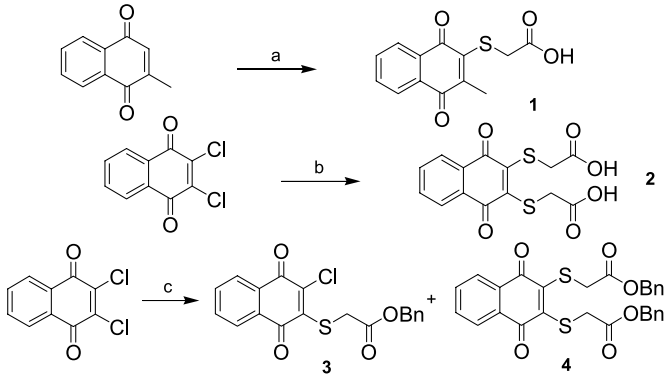

Scheme 1. Reagents and conditions: (a) HS–CH_2–CO_2H (1 equiv), DBU, ether, rt; (b) HS–CH_2–CO_2H (2 equiv), pyridine, toluene, 65 °C; (c) HS–CH_2–CO_2Bn (2 equiv), pyridine, toluene, 65 °C.

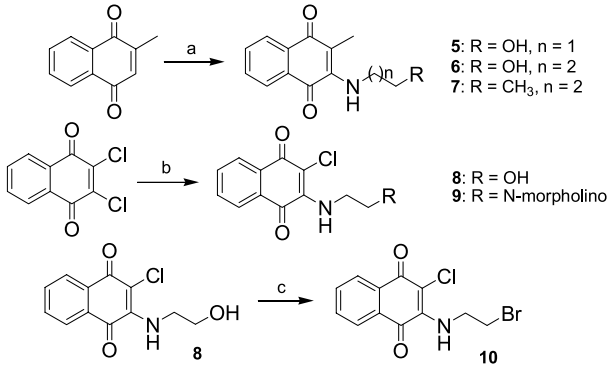

Scheme 2. Reagents and conditions: (a) R–NH_2, Et_2O, rt; (b) R–NH_2, Et_3N, Et_2O, rt; (c) CBr_4, PPh_3, anhydrous CH_2Cl_2, rt.

fluorescein diphosphate (FDP) as the substrate (Table 1). We synthesized Cpd 5 and NSC 95397, which were tested as references and showed, respectively, IC_{50} values of 3.65 and 3.77 μM under our assay conditions. Surprisingly, NSC 95397 gave an in vitro IC_{50} value in the micromolar range, although it was previously reported to inhibit CDC25B with a nanomolar concentration.[31] However, such discrepancies have already been reported for several CDC25 inhibitors of the naphthoquinone series.[35]

Table 1. In vitro inhibition of purified recombinant CDC25B3

	IC_{50} ± SD (μM)
Cpd 5	3.65 ± 0.2
NSC 95397	3.77 ± 0.9
1	4.13 ± 0.8
2	1.75 ± 0.1
3	3.95 ± 0.5
4	3.40 ± 0.3
5	8.85 ± 0.2
6	31.50 ± 9.9
7	≫100
8	15.40 ± 2.7
9	10.55 ± 0.4
10	10.50 ± 0.1

Enzyme inhibition was assayed on recombinant MBP-CDC25B3 protein using fluorescein 3,6-diphosphate as the substrate. The IC_{50} and the SD were calculated from at least three independent experiments with three determinations per tested concentration.

The four derivatives of the S-series **1**–**4** are the most potent in vitro CDC25B3 inhibitors with IC_{50} values ranging from 1.75 to 4.73 μM, similar or inferior to those of Cpd 5 and NSC 95397. The di-acid **2** and the di-ester **4** with IC_{50} values of 1.75 and 3.40 μM are slightly more potent CDC25 inhibitors than their mono-substituted analogs **1** and **3** with IC_{50} values of 4.13 and 3.95 μM, respectively. Thus, the replacement of the hydroxyl groups of Cpd 5 and NSC 95397 by carboxylic groups maintains the inhibitory potency but does not lead to the expected increase of activity.

To analyze the possible interactions of vitamin K_3 and compounds **1** and **2** with the catalytic domain of CDC25, molecular modeling was performed using the docking programs Surflex[36] and Ligandfit.[37] The docked poses with the most energetically favorable binding are shown in Figure 1. Our results obtained by both docking methods propose that vitamin K_3 binds in the inhibitor binding pocket defined by Kristjansdottir et al.[35] (Fig. 1A). In such a binding mode, vitamin K_3 is involved in strong vdW interactions with the pocket residues. In addition, a salt bridge between one oxygen of the naphthoquinone core and Arg482 was predicted by both Surflex and Ligandfit methods. Our docking experiments carried out with both programs suggest that compounds **1** (Fig. 1B) and **2** (Fig. 1C) bind into the active site and that the carboxylate group might occupy the phosphate binding pocket attracted by Arg479. Compound **2**, containing a second carboxylic group, could interact with Arg482 (proposed by Ligandfit) or Arg544 (proposed by Surflex) and form a salt bridge. We hypothesized that such a salt bridge should stabilize the binding of the ligand in the active site, thus higher activity of compound **2** in comparison with compound **1** should be expected, to a higher extent than experimentally observed.

The results of our docking experiments propose different binding modes for compounds **1** and **2** compared to vitamin K_3. The strong interaction of the carboxylate group of compounds **1** or **2** with Arg479 of the active site most likely brings the naphthoquinone core out of the floor of the inhibitor binding pocket. Presence of hydroxyl groups should not lead to such effects. Thus, a similar binding mode for vitamin K_3 and the hydroxyl

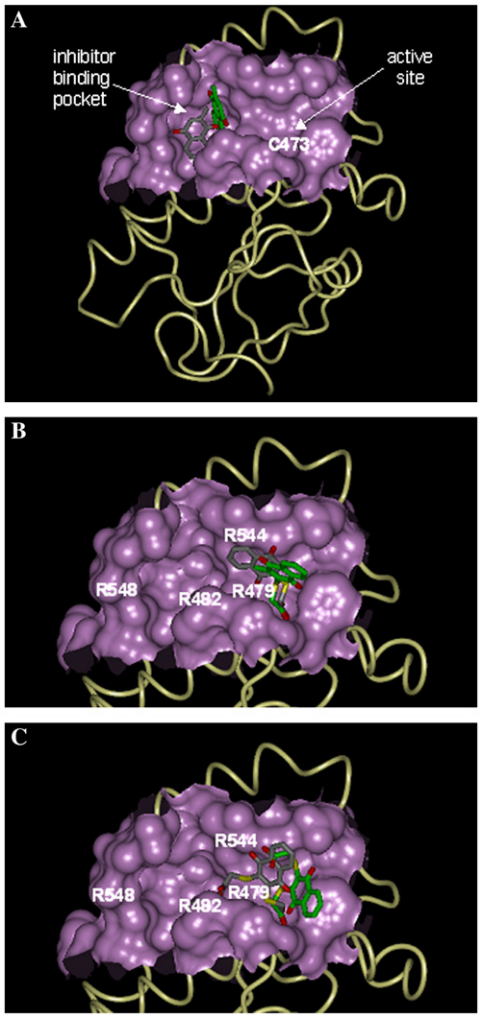

Figure 1. Molecular modeling. Inhibitor docked poses obtained with Surflex (in green) and Ligandfit (gray). CDC25B is shown as ribbon (white/yellow). The inhibitor binding pocket and the active site region are shown in purple. (A) Vitamin K_3; (B) compound **1**; and (C) compound **2**.

derivatives (Cpd 5 and NSC 95397) could be suggested. Hence, the hydroxyl and the carboxylic derivatives could interact differently with CDC25, and thus the substitution of hydroxyl (in Cpd 5 and NSC 95397) by carboxylic groups (in compounds **1** and **2**) does not lead to an increase in inhibitory activity.

The benzyl esters **3** and **4**, initially synthesized to improve cell penetration, were revealed to be as potent as their carboxylic free analogs **1** and **2**, supporting a different mode of binding for these compounds. In fact, if the carboxylic group of compounds **1** and **2** interacts just like the phosphate of CDK, as suggested by our modeling results, compounds **3** and **4** should not interact in the same way with CDC25. Finally, the introduction of a chlorine atom at position 2 (compound **3**), instead of a methyl group, had no significant effect on the inhibitory activity.

In the N-substituted series, replacement of the sulfur by a nitrogen atom, more conjugated to the quinone moiety than the sulfur atom, unfortunately led this second series of molecules to a low, but general, decrease of the inhibitory potency. Thus, the hydroxyl derivative **5** exhibited an IC_{50} value of 8.85 μM versus 3.65 μM for Cpd 5. Contrary to the sulfur derivatives, the replacement of the methyl group by a chlorine on the quinone moiety (compound **8**) significantly diminished the inhibitory activity (IC_{50} = 15.40 μM vs 8.85 μM for compound **5**). Increasing the length of the alkyl chain led to naphthoquinone **6**, which also showed a severe decrease of its inhibitory activity with an IC_{50} value of 31.50 μM. To evaluate the potential role of a hydrogen bond, the replacement of the terminal hydroxyl group by a methyl led to compound **7**, which showed no activity at doses up to 100 μM. The morpholino analog **9** was less potent than its parent compound NSC 663284 (IC_{50} = 0.2 μM on CDC25B2) with an IC_{50} value of 10.55 μM, confirming the importance of a quinolinedione nucleus.[25] Finally, replacement of the hydroxyl group of compound **6** by a bromine atom led to **10**, which interestingly showed an increase of activity with an IC_{50} value of 10.50 μM.

3.2. Cellular activity

The cytotoxicity of all compounds was evaluated on HeLa cells treated with increasing concentrations of inhibitors, using a WST-1 colorimetric test (Table 2). Cpd 5 and NSC 95397 were also tested under our assay conditions showing IC_{50} values of 8.8 and 10.8 μM, respectively. Most of our compounds displayed cytotoxic activity (IC_{50} values ranging from 3.5 to 30 μM), as expected for CDC25 inhibitors, the most active being the bromo derivative **10**. In the S-series, the benzyl ester derivatives **3** and **4**, prepared as prodrugs, were more cytotoxic than their free-carboxylic homologs **1** and **2** as expected. Thus, the di-acid **2** and its benzyl ester analog **4** showed IC_{50} values of 85.3 and 11.2 μM, respectively. We could also observe that the

Table 2. In vitro growth inhibition of HeLa cell line

	Antiproliferative assay IC_{50} ± SD (μM)	Clonogenic assay IC_{50} ± SD (μM)
Cpd 5	8.8 ± 3.8	4.1 ± 0.1
NSC 95397	10.8 ± 2.9	8.5 ± 0.7
1	17.8 ± 1.3	n.d.[a]
2	85.3 ± 6.0	n.d.[a]
3	9.6 ± 1.7	3.9 ± 0.6
4	11.2 ± 1.0	4.77 ± 1.3
5	25.7 ± 2.9	n.d.[a]
6	69.5 ± 20.1	n.d.[a]
7	>100 μM	n.d.[a]
8	22.7 ± 1.5	n.d.[a]
9	16.3 ± 3.2	n.d.[a]
10	3.5 ± 0.2	0.85 ± 0.1

Growth inhibition was assayed on HeLa cells using either the WST-1 cell proliferation assay or the crystal violet clonogenic assay. For the antiproliferative assay, the IC_{50} and the SD reported were calculated from at least three independent experiments with eight determinations per tested concentration. For the clonogenic assay, the IC_{50} and the SD reported were calculated from at least two independent experiments with two determinations per tested concentrations.

[a] Not determined.

mono-substituted naphthoquinones Cpd 5, **1**, and **3** were more efficient than the corresponding di-substituted analogs NSC 95397, **2**, and **4**. In the N-series, increasing the alkyl chain length induced a severe decrease of toxicity when compared to compound **5** (IC_{50} = 25.7 μM) and compound **6** (IC_{50} = 69.5 μM). Moreover, suppressing the terminal hydroxyl group led to **7**, which showed no cytotoxicity (IC_{50} > 100 μM), confirming the importance of a H-bond donor group to anchor the inhibitor in the catalytic domain of the enzyme. Finally, the replacement of the methyl group at position 3 on the quinone ring of compound **5** by a chlorine increased slightly the activity, as **8** has an IC_{50} of 22.7 μM. In conclusion, we could observe a correlation between in vitro inhibitory potency and antiproliferative activity of the synthesized compounds. Compound **10** displayed an antiproliferative activity higher than its in vitro phosphatase inhibitory activity, suggesting that it might trigger targets other than CDC25s. Indeed, the presence of the reactive bromomethyl group can lead to substitution reactions with nucleophilic species within the cells.

The effects on cell proliferation were further investigated in a clonogenic assay for the more cytotoxic compounds, namely compounds **3**, **4**, and **10** (Table 2). HeLa cells were treated at day 1 with increasing concentrations of drugs and then plated for 10 additional days. After crystal violet staining and colony counting, dose–response curves were drawn and the IC_{50} was determined. Each of the tested compounds was effective at inhibiting clonal proliferation of the HeLa cells in a concentration-dependent manner with IC_{50} ranging from 0.85 to 8.5 μM, the most potent being the bromo derivative **10** with a submicromolar IC_{50} value. As in the proliferation assay, the mono-substituted derivatives Cpd 5 and compound **3** exhibited IC_{50} values of 4.1 and 3.9 μM inferior to those of the di-substituted NSC 95397 and compound **4**, which showed, respectively, IC_{50} values of 8.5 and 4.77 μM. Moreover, the three tested compounds **3**, **4**, and **10** were more potent than NSC 95397.

3.3. Molecular characterization of the cellular effects

Inhibition of CDC25 phosphatases should induce the accumulation of the hyperphosphorylated form of their natural substrate, namely the CDK kinases. As CDK1 (Cdc2) tyrosine 15 phosphorylation is experimentally accessible, we investigated the molecular basis of the inhibitory activity of our compounds by monitoring, on HeLa cells, the effect of compound **1** on this phosphorylation status. HeLa cells were treated with increasing concentrations of compound **1** for 8 h, lysed, and processed for Western blot analysis using an antibody directed against the 15-phosphorylated tyrosine form of the CDK kinases. Actin was used as loading control. As shown in Figure 2, compound **1** at 10 μM induced a moderate accumulation of the 15-phosphorylated tyrosine form of CDK in a concentration-dependent manner. The inhibition of CDK dephosphorylation suggests that compound **1** down-regulates the phosphatase activity of CDC25 toward these kinases, indicating that treatment with this drug

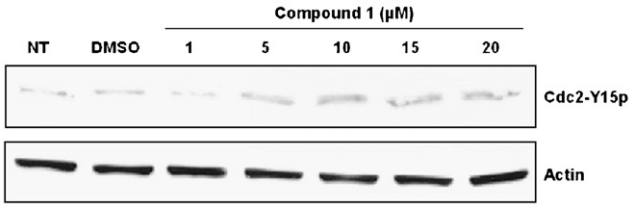

Figure 2. Effect of compound **1** on CDK phosphorylation status. After treatment with compound **1** at the indicated concentrations for 8 h, HeLa cells were lysed and processed for Western blot analysis using antibodies against tyrosine 15-phosphorylated CDKs and actin. Phospho-cdc2 (Tyr15) detects endogenous levels of Cdc2, CDK1, and CDK5 only when phosphorylated at tyrosine 15.

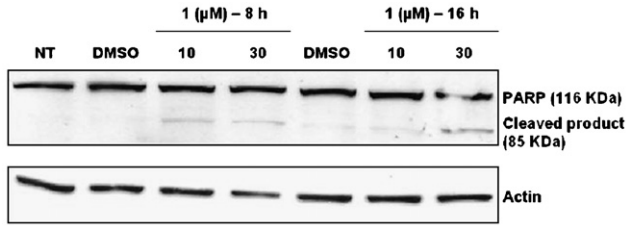

Figure 3. Effect of compound **1** on apoptosis. After treatment with compound **1** at the indicated concentrations for 8 or 16 h, HeLa cells were lysed and processed for Western blot analysis using antibodies against full and cleaved PARP and actin.

inhibits CDC25 phosphatase activity in these cells. The effect of this compound on cell cycle progression was therefore examined.

HeLa cells were used to investigate the effect of compounds **1** and **10** on cell cycle progression by flow cytometry determination of their DNA content after propidium iodide staining. After 24 h of treatment with 10 μM of inhibitor, a concentration that inhibited proliferation (Table 2), the cell cycle distribution was only modestly affected with a slight increase in cells containing a G_2 DNA content, suggesting that the cells treated with either compound **1** or **10** were arrested at various stages of the cell cycle (data not shown).

As we noticed that compound **1** induced a high level of mortality on HeLa cells at high concentration, we investigated whether cell death occurred through an apoptosis process by monitoring the cleavage of poly-(ADP-ribose)-polymerase (PARP). This death substrate is a final common pathway of drug-induced apoptosis and is specifically cleaved during apoptosis to produce a 85 kDa fragment.[38] As shown in Figure 3, both concentrations of compound **1** induced cleavage of the 116 kDa polypeptide to the 85 kDa fragment after 8 h of treatment.

4. Conclusion

In conclusion, we have developed two new series of vitamin K_3 derivatives that exhibited in vitro inhibition of CDC25 activity in the low micromolar range. The introduction of a carboxylic group, bioisostere of the

phosphate, did not significantly increase the CDC25 inhibitory activity (compounds **1** and **2**). The corresponding esters **3** and **4** proved to be interesting, as they were as potent as their carboxylic analogs, suggesting a different way of interacting with the enzyme. The substitution of the alkyl chain also seemed to be essential, as removing a H-bond donor group led to a decrease of activity that may be linked to a loss of a hydrogen bond (compounds **6/7**). As compound **10** exhibited the best antiproliferative activity but might inhibit targets other than CDC25s, it will be further investigated. Finally, we could observe that compound **1** caused increased phosphorylation of CDK, indicating that the CDC25 phosphatase family is, at least, one of the targets of our compounds and that it induced the cleavage of PARP, indicating that apoptosis was triggered by this molecule.

5. Experimental

5.1. Abbreviations

DBU, 1,8-diazabicyclo[5.4.0]undec-7-ene; DMF, dimethylformamide; DMSO, dimethylsulfoxide; TEA, triethylamine; and TFA, trifluoroacetic acid.

5.2. Chemicals

The intermediates 2-(naphthyl)ethyl bromide[39] and benzyl (2-methylthio)acetate,[40] as well as the final compounds Cpd 5[30] and NSC 95397,[33] were synthetized according to reported procedures. All other chemicals were purchased from Acros and Aldrich, and used without further purification unless otherwise specified.

5.3. General

All melting points were determined with the Kofler apparatus and are uncorrected. Analytical thin-layer chromatography was performed on Kieselgel $60F_{254}$ plates (Merck). Spots were visualized under UV (254 nm). Flash chromatography was performed on silica gel 60 (0.04–0.063 mm) purchased from Carlo Erba–SDS. ^{1}H NMR and ^{13}C NMR spectra were recorded on a Bruker WMFT-250 MHz spectrometer. Chemical shifts were expressed in parts per million (ppm) using TMS as internal standard. Mass spectra were recorded on a Bruker Esquire 3000 Ion Trap spectrometer using an electrospray source at the Laboratoire de Chimie Structurale Organique et Biologique, Université Pierre et Marie Curie, Paris, France. Elemental analyses (C, H, and N), performed at the Service de Microanalyse, Pierre et Marie Curie Université, Paris, France, were within ±0.4% of the theoretical values.

5.4. (3-Methyl-1,4-dioxo-1,4-dihydronaphthalen-2-ylsulfanyl) acetic acid (1)

Compound **1** was obtained according to published procedure.[30] DBU (0.02 mL, 0.14 mol) was added to a solution of 2-methyl-[1,4]-naphthoquinone (1 g, 5.8 mmol) and mercaptoacetic acid (0.4 mL, 5.8 mmol) in ether (30 mL). The solution turned red and the stirring was maintained for 12 h at room temperature. HCl 3.6 M (4 mL) was then added and the aqueous phase was extracted with ether (2 × 20 mL). The organic layers were combined, dried (Na_2SO_4), and the solvent was evaporated under reduced pressure. The residue was purified by flash chromatography (EtOAc/cyclohexane, 3:7) to give **1** as an orange powder (638 mg, 42%); mp: 156 °C; ^{1}H NMR ($CDCl_3$): δ 8.09–8.04 (2H, m, H_5 and H_8), 7.73–7.65 (2H, m, H_6 and H_7), 3.96 (2H, s, CH_2), 2.36 (3H, s, CH_3). Anal. Calcd for $C_{14}H_{10}O_6S_2$: C, 59.54; H, 3.81. Found: C, 59.44; H, 4.16.

5.5. (3-Carboxymethylsulfanyl-1,4-dioxo-1,4-dihydronaphthalen-2-ylsulfanyl) acetic acid (2)

Compound **2** was prepared following a reported procedure with minor modifications.[33] Pyridine (0.8 mL) was added to a solution of 2,3-dichloro-[1,4]-naphthoquinone (1 g, 4.4 mmol) and mercaptoacetic acid (0.70 mL, 10.12 mmol) in toluene (16 mL) heated at 55 °C. After pyridine addition, the temperature increased and was maintained at 65 °C. Within 15 min, a red precipitate formed. The reaction mixture was then cooled to room temperature, filtered, and the precipitate rinsed with water before being purified by flash chromatography (CH_2Cl_2/MeOH/AcOH, 95:5:2) to give **2** as a red powder (1.31 g, 89%); mp: 194 °C; ^{1}H NMR (DMSO-d_6): δ 8.02–7.99 (2H, m, H_5 and H_8), 7.89–7.86 (2H, m, H_6 and H_7), 4.13 (4H, s, 2× S–CH_2); ^{13}C NMR (DMSO-d_6): δ 178.63 (2C), 170.23 (2C), 145.67 (2C), 134.28 (2C), 132.78 (2C), 126.83 (2C), 35.98 (2C). Anal. Calcd for $C_{14}H_{10}O_6S_2 \cdot 0.5H_2O$: C, 48.41; H, 3.17. Found: C, 48.11; H, 3.12.MS (ESI) *m*/*z* 339 $(M+1)^+$.

5.6. (3-Chloro-1,4-dioxo-1,4-dihydronaphthalen-2-ylsulfanyl) acetic acid benzyl ester (3) and (3-benzyloxycarbonyl-methylsulfanyl-1,4-dioxo-1,4-dihydronaphthalen-2-ylsulfanyl) acetic acid benzyl ester (4)

Pyridine (0.66 mL) was added to a solution of 2,3-dichloro-[1,4]-naphthoquinone (820 mg, 3.6 mmol) and benzyl mercaptoacetate (1.5 g, 7.2 mmol) heated at 55 °C in toluene (20 mL). The solution was heated at 55 °C for 1 h, cooled to room temperature, and filtered. The filtrate was evaporated under reduced pressure and purified by flash chromatography (EtOAc/cyclohexane, 1:9) to provide **3** as a yellow powder (564 mg, 42%); mp: 108 °C. ^{1}H NMR ($CDCl_3$): δ 8.14–8.11 (1H, m, H_5), 8.01–7.98 (1H, m, H_8), 7.79–7.70 (2H, m, H_6 and H_7), 7.29–7.27 (5H, m, Hphenyl), 5.14 (2H, s, CH_2), 4.21 (2H, s, S–CH_2); ^{13}C NMR (DMSO-d_6): δ 179.54, 174.82, 168.72, 147.47, 139.06, 135.85, 134.76, 134.59, 132.61, 131.00, 128.67 (2C), 128.49, 128.36 (2C), 127.31, 126.97, 67.00, 35.10. Anal. Calcd for $C_{19}H_{13}ClO_4S$: C, 61.21; H, 3.50. Found: C, 61.01; H, 3.37. MS (ESI) *m*/*z* 373.2 $(M+1)^+$. Compound **4** was isolated as a red powder (681 mg, 36%); mp: 90 °C; ^{1}H NMR ($CDCl_3$): δ 7.98–7.94 (2H, m, H_5 and H_8), 7.70–7.66 (2H, m, H_6 and H_7), 7.28 (10H, m, Hphenyl), 5.14 (4H, s, 2× CH_2), 4.07 (4H, s, 2× S–CH_2); ^{13}C NMR (DMSO-d_6): δ 178.51 (2C), 168.82 (2C), 145.74

(2C), 135.88 (2C), 134.31 (2C), 132.62 (2C), 128.66 (3C), 128.41 (2C), 128.35 (3C), 126.87 (2C), 66.90 (2C), 35.52 (2C). Anal. Calcd for $C_{28}H_{22}O_6S_2$: C, 64.86; H, 4.25. Found: C, 64.72; H, 4.12. MS (ESI) *m/z* 519 $(M+1)^+$.

5.7. 2-(2-Hydroxyethyl)amino-3-methyl-[1,4]-naphthoquinone (5)

Compound **5** was obtained according to published procedure[41] from 3-methyl-[1,4]-naphthoquinone (0.5 g, 2.9 mmol) and ethanolamine (0.18 mL, 2.9 mmol) as an orange powder (160 mg, 24%); mp: 131 °C; ^{1}H NMR (DMSO-d_6): δ 7.89 (2H, m, H_5 and H_8), 7.78–7.63 (2H, m, H_6 and H_7), 6.47 (1H, br s, NH), 4.90 (1H, br s, OH), 3.59 (4H, m, 2× CH_2), 2.09 (3H, s, CH_3); ^{13}C NMR (DMSO-d_6): δ 182.43, 182.05, 147.19, 134.69, 133.09, 132.37, 130.55, 125.90, 125.70, 111.19, 60.80, 47.12, 11.05.

5.8. 2-(3-Hydroxypropyl)amino-3-methyl-[1,4]-naphthoquinone (6)

Compound **6** was obtained according to published procedure[41] from 3-methyl-[1,4]-naphthoquinone (1.5 g, 8.72 mmol) and propanolamine (0.67 mL, 8.71 mmol) as a dark red powder (410 mg, 20%); mp: 74 °C; ^{1}H NMR ($CDCl_3$): δ 8.11 (1H, d, J = 7.6 Hz, H_5), 8.01 (1H, d, J = 7.5 Hz, H_8), 7.73–7.56 (2H, m, H_6 and H_7), 5.75 (1H, br s, NH), 3.62–3.54 (2H, m, N–CH_2), 2.27 (3H, s, CH_3), 1.71–1.63 (2H, m, CH_2), 1.53–1.41 (2H, m, CH_2), 0.99 (3H, t, J = 7.2 Hz, CH_3); ^{13}C NMR (DMSO-d_6): δ 182.46, 181.96, 147.00, 134.68, 133.13, 132.31, 130.52, 125.87, 125.68, 110.84, 58.97, 42.75, 33.64, 10.98.

5.9. 2-Butylamino-3-methyl-[1,4]-naphthoquinone (7)

Compound **7** was prepared according to published procedure[41] from 3-methyl-[1,4]-naphthoquinone (1.5 g, 8.72 mmol) and butylamine (0.86 mL, 8.71 mmol) as a dark red powder (576 mg, 27%); mp: 79 °C; ^{1}H NMR ($CDCl_3$): δ 8.10 (1H, d, J = 7.5 Hz, H_5), 8.01 (1H, d, J = 7.5 Hz, H_8), 7.72–7.56 (2H, m, H_6 and H_7), 5.98 (1H, br s, NH), 3.87–3.72 (4H, m, O–CH_2 and N–CH_2), 2.26 (3H, s, CH_3), 1.98–1.88 (2H, m, CH_2); ^{13}C NMR (DMSO-d_6): δ 182.46, 181.87, 146.82, 134.63, 133.09, 132.27, 130.53, 125.85, 125.65, 110.95, 44.49, 33.07, 19.71, 14.00, 10.92.

5.10. 2-Chloro-3-(2-hydroxyethyl-amino)-[1,4]-naphthoquinone (8)

Compound **8** was obtained according to published procedure[42,43] from 2,3-dichloro-[1,4]-naphthoquinone (0.5 g, 2.2 mmol) and ethanolamine (0.18 mL, 2.2 mmol) in the presence of TEA (0.3 mL, 2.2 mmol) as an orange powder (257 mg, 46%); mp: 147 °C; ^{1}H NMR ($CDCl_3$): δ 8.17 (d, 1H, J = 7.8 Hz, H_5), 8.05 (1H, d, J = 7.5 Hz, H_8), 7.78–7.62 (m, 2H, H_6 and H_7), 6.43 (1H, br s, NH), 4.11–4.05 (2H, m, O–CH_2), 3.93–3.91 (2H, m, N–CH_2); ^{13}C NMR (DMSO-d_6): δ 180.44, 175.74, 145.97, 135.21, 132.97, 132.33, 131.69, 130.23, 126.80, 126.14, 60.71, 46.66.

5.11. 2-Chloro-3-[2-(morpholin-4-yl)ethylamino]-[1,4]-naphthoquinone (9)

To a suspension of 2,3-dichloro-[1,4]-naphthoquinone (1 g, 4.4 mmol) in ether (40 mL) were added 2-aminoethylmorpholine (0.6 mL, 4.4 mmol) and TEA (0.61 mL, 1 equiv). The reaction mixture was stirred at room temperature for 12 h, concentrated under reduced pressure, diluted with ethyl acetate, and washed with water. The organic layer was dried (Na_2SO_4) and the solvent was evaporated in vacuo. The residue was purified by flash chromatography (EtOAc/cyclohexane, 1:1) to give **9** as an orange powder (830 mg, 59%); mp: 112 °C; ^{1}H NMR ($CDCl_3$): δ 8.17 (1H, d, J = 8.6 Hz, H_5), 8.05 (1H, d, J = 9.6 Hz, H_8), 7.77–7.64 (m, 2H, H_6 and H_7), 6.90 (1H, br s, NH), 3.99 (2H, m, O–CH_2), 3.78 (4H, t, J = 4.55 Hz, 2× O–CH_2morpholine), 2.70 (2H, t, J = 6 Hz, N–CH_2), 2.55 (4H, t, J = 4.55 Hz, 2× N–CH_2morpholine); ^{13}C NMR (DMSO-d_6): δ 180.37, 175.56, 146.11, 135.20, 132.98, 132.31, 130.31, 126.82, 126.13, 66.58 (2C), 57.80, 53.20 (2C), 41.08. Anal. Calcd for $C_{16}H_{17}ClN_2O_3$: C, 59.90; H, 5.30; N, 8.73. Found: C, 60.09; H, 5.33; N, 8.61. MS (ESI) *m/z* 321 $(M+1)^+$.

5.12. 2-(2-Bromoethylamino)-3-chloro-[1,4]-naphthoquinone (10)

Compound **10** was obtained according to the procedure described by Nishizawa et al.[34] To a mixture of **8** (1 g, 4 mmol) and CBr_4 (2 g, 6 mmol) dissolved in anhydrous CH_2Cl_2 (70 mL), PPh_3 (1.26 g, 4.8 mmol) was added portionwise. The reaction mixture was stirred at room temperature for 2 h. The organic phase was washed with water (3 × 50 mL), dried (Na_2SO_4), and the solvent was evaporated under reduced pressure. The crude residue was purified by flash chromatography (EtOAc/cyclohexane, 1:5) to give **10** as an orange powder (909 mg, 72%); mp: 180 °C; ^{1}H NMR ($CDCl_3$): δ 8.18 (1H, d, J = 7.5 Hz, H_5), 8.08 (1H, d, J = 7.7 Hz, H_8), 7.80–7.64 (2H, m, H_6 and H_7), 6.33 (1H, br s, NH), 4.27 (2H, m, CH_2Br), 3.64 (2H, t, J = 6 Hz, N–CH_2); ^{13}C NMR (DMSO-d_6): δ 180.37, 175.83, 145.50, 135.18, 133.16, 132.01, 130.39, 126.88, 126.13, 45.56, 32.69. Anal. Calcd for $C_{12}H_9BrClNO_2$: C, 45.78; H, 2.86; N, 4.45. Found C, 45.67; H, 2.93; N, 4.43. MS (ESI) *m/z* 316 $(M+1)^+$.

5.13. Enzymes, cell culture, chemicals, and antibodies

The maltose binding protein-CDC25B3 recombinant protein was produced in bacteria, as previously described.[27] The human cancer cell line HeLa was obtained from Aptanomics (Lyon, France). Cells were cultured at 37 °C in Dulbecco's minimum essential medium complemented with 10% fetal bovine serum and 100 U/mL penicillin/streptomycin in a humidified atmosphere of 5% CO_2. The CDC25 inhibitors were solubilized in dimethylsulfoxide so that the DMSO final concentration was <0.1%. The tetrazolium salt WST-1 was purchased from Roche Diagnostics (Mannheim, Germany). The following antibodies were used in this study: phospho-cdc2(Tyr15) antibody was purchased from Cell Signaling Technology (Beverly, MA), human full and cleaved

α-PARP antibody from BD Pharmingen (San Jose, CA), actin antibody from Sigma (St. Louis, MO), and the secondary antibodies, namely anti-rabbit and anti-mouse IgG-horseradish peroxidase antibodies, from Amersham Biosciences (Buckinghamshire, England).

5.14. In vitro enzymatic assay

The activity of the MBP-CDC25B3 recombinant enzyme was monitored using fluorescein diphosphate. The assay was performed in 96-well plates in a final volume of 200 μL. The maltose binding protein-CDC25B3 was kept in elution buffer [50 mM phosphate, pH 7.5, 300 mM NaCl, 500 mM imidazole, and 10% glycerol]. It was diluted in assay buffer [30 mM Tris–HCl (pH 8.2), 75 mM NaCl, 0.67 mM EDTA, 0.033% BSA, and 1 mM DTT]. The final concentration of CDC25B3 was 75 ng/well. Products were studied in concentration response up to 100 μM. The reaction was initiated by addition of 30 μM fluorescein diphosphate, followed by an immediate measurement of fluorescein monophosphate emission with a Fluoroskan Ascent (Lab Systems; excitation filter: 485 nm, emission filter: 530 nm). The results are expressed as means of at least three independent experiments with three determinations per tested concentration and per experiment. For each compound, the drug concentration required for 50% inhibition (IC_{50}) was determined from a sigmoidal dose–response curve using GraphPad Prism (GraphPad Software, San Diego, CA).

5.15. Cell proliferation assay

The inhibition of cell proliferation was determined using a WST-1 colorimetric assay based on the cleavage of the tetrazolium salt WST-1 by mitochondrial dehydrogenases in viable cells, leading to formazan formation. At day 0, HeLa cells were plated at 3000 cells/well in 96-well tissue culture plates with 95 μL medium/well. At day 1, cells were treated for 96 h with 5 μL of increasing concentrations of drug (up to 100 μM). At day 6, 10 μL of WST-1 was added per well, and cells were incubated for 2 h at 37 °C in a humidified atmosphere of 5% CO_2. Absorbance was measured at 430 nm. The results are expressed as means of at least three independent experiments with eight determinations per tested concentration and per experiment. For each compound, the IC_{50} was determined from a sigmoidal dose–response using GraphPad Prism (GraphPad Software, San Diego, CA).

5.16. Clonogenic assay

For cloning inhibition assays, HeLa cells were plated at 100 cells/well in six-well tissue culture plates with 2.5 mL medium/well. After 24 h growth at 37 °C in a humidified atmosphere of 5% CO_2, the culture medium was replaced by control medium or medium containing inhibitors at increasing concentrations (up to 100 μM) and incubated for 10 days. Cells were then washed with phosphate-buffered saline and fixed in 10% formaldehyde for 30 min at room temperature. They were carefully rinsed with water, stained with 1 mL crystal violet (2 g in 100 mL ethanol, then 2 mL in 100 mL water) for 30 min, and finally rinsed with water. The plating efficiency was determined by counting the colonies. The results are expressed as means of two independent experiments for Cpd 5 and NSC 95397 and as means of three independent experiments for **3**, **4**, and **10**. For each compound, the IC_{50} was determined from a sigmoidal dose–response using GraphPad Prism (GraphPad Software, San Diego, CA).

5.17. Immunoblotting

HeLa cells were plated at 2×10^6 cells on a 10 cm plate and incubated for 24 h. They were treated with 1, 5, 10, 15, and 20 μM compound **1** for 8 h for experiments concerning the phosphorylation status of Cdc2. As far as apoptosis is concerned, cells were treated with 10 and 30 μM compound **1** for 8 and 16 h. Cells were washed four times with ice-cold phosphate-buffered saline and lysed in 250 μL lysis buffer [50 mM HEPES, pH 7.5, 1% Triton X-100, 150 mM NaCl, 10% glycerol, 1 mM $MgCl_2$, 1 mM EGTA, phosphatase inhibitor (5 mM Na_3VO_4), kinase inhibitor (10 mM NaF), and protease inhibitor (1 mM phenylmethylsulfonyl fluoride and Complete™ protease inhibitors mixture, Roche Molecular Biochemicals)]. After a 15-min incubation at 4 °C, the lysates were collected and centrifuged at 13,200*g* for 10 min at 4 °C to remove insoluble material. Protein concentration of the lysates was determined using the Bradford assay (Sigma). Lysate proteins (25 μg/lane for Cdc2 and 50 μg/lane for PARP) were separated on a 12% (Cdc2) or 10% (PARP) gel by SDS–polyacrylamide gel electrophoresis and electroblotted onto a nitrocellulose membrane. Membranes were saturated overnight at 4 °C with Superblock buffer (Pierce) and blotted for 1 h at room temperature with the appropriate primary antibody: rabbit polyclonal anti-phospho-Cdk1 diluted at 1:2000, mouse monoclonal full and cleaved anti-PARP diluted at 1:1000, and mouse monoclonal anti-actin diluted at 1:10,000. After four washes with TBS–0.1% Tween, membranes were incubated with the secondary antibody (horseradish peroxidase-conjugated anti-rabbit or anti-mouse IgG diluted at 1:10,000) for 30 min at room temperature. Immunoreactive bands were detected using the ECL immunodetection system (Amersham Biosciences). The results are expressed as means of at least three independent experiments.

5.18. Molecular modeling studies

The crystal structure of the catalytic subunit of CDC25B (PDB code 1CWT) was used to dock vitamin K_3 and the compounds **1** and **2** in CDC25. All docking calculations were carried out with Surflex[36] and Ligandfit.[37] The program Surflex defines a binding site called a protomol tuned to produce a docking target consistent with the binding pocket properties. Flexible docking of the ligand was performed with the incremental construction algorithm as described. The best 10 poses for each ligand were ranked by using the Surflex scoring function involving hydrophobic, polar, entropic, and solvation terms. The best energy ranked pose was selected. The

calculations were run on a Xeon 3.0 GHz Linux Dell Workstation. The Ligandfit approach combines a shape comparison filter and a Monte Carlo conformational search. The calculations were performed using the CFF 1.02 force field. The binding site region of CDC25 was determined with the implemented cavity search algorithm in Ligandfit. Binding site partitioning (2 partitions) was used to dock the flexible ligand. Rigid body minimization (100 steps) was performed for each pose, followed by a 50-step ligand-flexible minimization. The best 20 poses for each ligand were saved and the best energy-ranked pose was selected by using the Ligandfit docking/scoring function involving vdW interactions and a distance-dependent electrostatic function. The calculations were carried out on a SGI Fuel workstation. The figures were obtained using the program InsightII (Accelrys, San Diego, CA).

Acknowledgment

We thank la Ligue Nationale contre le Cancer for its financial support (Equipes ''labellisées'').

References and notes

1. Honda, R.; Ohba, Y.; Nagata, A.; Okayama, H.; Yasuda, H. *FEBS Lett.* **1993**, *318*, 331.
2. Strausfeld, U.; Labbe, J. C.; Fesquet, D.; Cavadore, J. C.; Picard, A.; Sahdu, K.; Russell, P.; Doree, M. *Nature* **1991**, *351*, 242.
3. Galaktionov, K.; Beach, D. *Cell* **1991**, *67*, 1181.
4. Sadhu, K.; Reed, S. I.; Richardson, H.; Russell, P. *Proc. Natl. Acad. Sci. U.S.A.* **1990**, *87*, 5139.
5. Nagata, A.; Igarashi, M.; Jinno, S.; Suto, K.; Okayama, H. *New Biol.* **1991**, *3*, 959.
6. Forrest, A. R.; McCormack, A. K.; DeSouza, C. P.; Sinnamon, J. M.; Tonks, I. D.; Hayward, N. K.; Ellem, K. A.; Gabrielli, B. G. *Biochem. Biophys. Res. Commun.* **1999**, *260*, 510.
7. Baldin, V.; Cans, C.; Superti-Furga, G.; Ducommun, B. *Oncogene* **1997**, *14*, 2485.
8. Hoffmann, I.; Draetta, G. F.; Karsentti, E. *EMBO J.* **1994**, *13*, 4302.
9. Jinno, S.; Suto, J.; Nagata, A.; Igarashi, M.; Kanaoka, Y.; Nojima, H.; Okayama, H. *EMBO J.* **1994**, *13*, 1549.
10. Molinari, M.; Mercurilo, C.; Dominguez, J.; Goubin, F.; Draetta, G. F. *EMBO Rep.* **2000**, *1*, 71.
11. Lammer, C.; Wagerer, S.; Saffrich, R.; Mertens, D.; Ansorge, W.; Hoffmann, I. *J. Cell Sci.* **1998**, *111*, 2445.
12. Millar, J. B.; Blewitt, J.; Gerace, L.; Sadku, K.; Featherstone, C.; Russell, P. *Proc. Natl. Acad. Sci. U.S.A.* **1991**, *88*, 10500.
13. Galaktionov, K.; Lee, A. K.; Eckstein, J.; Draetta, G.; Meckler, J.; Loda, M.; Beach, D. *Science* **1995**, *269*, 1575.
14. Gasparotto, D.; Maestro, R.; Piccinin, S.; Vukosavljevic, T.; Barzan, L.; Sulfaro, L.; Boiocchi, M. *Cancer Res.* **1997**, *57*, 2366.
15. Wu, W.; Fan, Y. H.; Kemp, B. L.; Walsh, G.; Mao, L. *Cancer Res.* **1998**, *58*, 4082.
16. Hernandez, S.; Hernandez, L.; Bea, S.; Cazorla, M.; Fernandez, P. L.; Nadal, A.; Muntane, J.; Mallofre, C.; Montserrat, E.; Cardesa, A.; Campo, E. *Cancer Res.* **1998**, *58*, 1762.
17. Takahashi, M.; Dodo, K.; Sugimoto, Y.; Aoyagi, Y.; Yamada, Y.; Hashimoto, Y.; Shirai, R. *Bioorg. Med. Chem. Lett.* **2000**, *10*, 2571.
18. Cebula, R. E.; Blanchard, J. L.; Boisclair, M. D.; Pal, K.; Bockovich, N. J. *Bioorg. Med. Chem. Lett.* **1997**, *7*, 2015.
19. Chen, C.; Liu, Y. Z.; Shia, K. S.; Tseng, H. Y. *Bioorg. Med. Chem. Lett.* **2002**, *12*, 2729.
20. Kar, S.; Lefterov, I. M.; Wang, M.; Lazo, J. S.; Scott, C. N.; Wilcox, C. S.; Carr, B. I. *Biochemistry* **2003**, *42*, 10490.
21. Dodo, K.; Takahashi, M.; Yamada, Y.; Sugimoto, Y.; Hashimoto, Y.; Shirai, R. *Bioorg. Med. Chem. Lett.* **2000**, *10*, 615.
22. Shimazawa, R.; Suzuki, T.; Dodo, K.; Shirai, R. *Bioorg. Med. Chem. Lett.* **2004**, *14*, 3291.
23. Ham, S. W.; Park, J.; Lee, S.-J.; Kim, W.; Kang, K.; Choi, K. H. *Bioorg. Med. Chem. Lett.* **1998**, *8*, 2507.
24. Wang, Z.; Southwick, E. C.; Wang, M.; Kar, S.; Rosi, K. S.; Wilcox, C. S.; Lazo, J. S.; Carr, B. I. *Cancer Res.* **2001**, *61*, 7211.
25. Lazo, J. S.; Aslan, D. C.; Southwick, E. C.; Cooley, K. A.; Ducruet, A. P.; Joo, B.; Vogt, A.; Wipf, P. *J. Med. Chem.* **2001**, *44*, 4042.
26. Brisson, M.; Nguyen, Y.; Vogt, A.; Yalowich, J.; Giorgianni, A. M.; Tobi, D.; Bahar, I.; Stephenson, C. R.; Wipf, P.; Lazo, J. S. *Mol. Pharmacol.* **2004**, *66*, 824.
27. Brezak, M. C.; Quaranta, M.; Mondésert, O.; Galcera, M. O.; Lavergne, O.; Alby, F.; Cazales, M.; Baldin, V.; Thurieau, C.; Harnett, J.; Lanco, C.; Kasprzyk, P. G.; Prevost, G. P.; Ducommun, B. *Cancer Res.* **2004**, *64*, 3320.
28. Contour-Galcera, M. O.; Lavergne, O.; Brezak, M. C.; Ducommun, B.; Prevost, G. *Bioorg. Med. Chem. Lett.* **2004**, *14*, 5809.
29. Nishikawa, Y.; Carr, B. I.; Wang, M.; Kar, S.; Finn, F.; Dowd, P.; Zheng, Z. B.; Kerns, J.; Naganathan, S. *J. Biol. Chem.* **1995**, *270*, 28304.
30. Tamura, K.; Southwick, E. C.; Kerns, J.; Rosi, K.; Carr, B. I.; Wilcox, C.; Lazo, J. S. *Cancer Res.* **2000**, *60*, 1317.
31. Lazo, J. S.; Nemoto, K.; Pestell, K. E.; Cooley, K.; Southwick, E. C.; Mitchell, D. A.; Furey, W.; Gussio, R.; Zaharevitz, D. W.; Joo, B.; Wipf, P. *Mol. Pharmacol.* **2002**, *61*, 720.
32. Reynolds, R. A.; Yem, A. W.; Wolfe, C. L.; Delbel, J. M. R.; Chidester, C. G.; Watenpaugh, K. D. *J. Mol. Biol.* **1999**, *293*, 559.
33. Kulka, M. *Can. J. Chem.* **1962**, *40*, 1235.
34. Nishizawa, S.; Cui, Y. Y.; Minagawa, M.; Morita, K.; Kato, Y.; Taniguchi, Y.; Kato, R.; Teramae, N. *J. Chem. Soc., Perkin Trans. 2* **2002**, 866.
35. Kristjansdottir, K.; Rudolph, J. *Chem. Biol.* **2004**, *11*, 1043.
36. Jain, A. N. *J. Med. Chem.* **2003**, *46*, 499–511.
37. Venkatachalam, C. M.; Jiang, X.; Oldfield, T.; Waldman, M. *J. Mol. Graphics Modell.* **2003**, *21*, 289–307.
38. Kaufmann, S. H.; Desnoyers, S.; Ottaviano, Y.; Davidson, N. E.; Poirier, G. G. *Cancer Res.* **1993**, *53*, 3976–3985.
39. Campaigne, E.; Heaton, B. G. *J. Org. Chem.* **1964**, *29*, 2372.
40. Woulfe, S. R.; Miller, M. J. *J. Org. Chem.* **1986**, *51*, 3133.
41. Nakai, N.; Hase, J. I. *Chem. Pharm. Bull.* **1968**, *16*, 2334.
42. Ohta, S.; Hinata, S.; Kawasaki, I.; Yamashita, M. *Chem. Pharm. Bull.* **1994**, *42*, 2360.
43. Prescott, B. *J. Med. Chem.* **1969**, *12*, 181.